Biochimica et Biophysica Acta 821 (1985) 243–252
Elsevier

BBA 72822

Target analysis studies of red cell water and urea transport

James A. Dix [a], D.A. Ausiello [b], C.Y. Jung [c] and A.S. Verkman [d,*]

[d] *Division of Nephrology, 1065 HSE, University of California, San Francisco, CA 94143,* [a] *Department of Chemistry, State University of New York, Binghamton, NY 13901,* [b] *Renal Unit, Massachusetts General Hospital, Boston, MA 02114, and* [c] *Department of Biophysics, State University of New York, Buffalo, NY 14215 (U.S.A.)*

(Received January 30th, 1985)
(Revised manuscript received August 1st, 1985)

Key words: Target analysis; Water; Urea transport; (Erythrocyte)

Radiation inactivation was used to determine the nature and molecular weight of water and urea transporters in the human red cell. Red cells were frozen to −50°C in a cryoprotectant solution, irradiated with 1.5 MeV electrons, thawed, washed and assayed for osmotic water and urea permeability by stopped-flow light scattering. The freezing and thawing process did not affect the rates of water or urea transport or the inhibitory potency of *p*-chloromercuribenzenesulfonate (pCMBS) on water transport and of phloretin on urea transport. Red cell urea transport inactivated with radiation (0–4 Mrad) with a single target size of 469 ± 36 kDa. 40 μM phloretin inhibited urea flux by approx. 50% at each radiation dose, indicating that urea transporters surviving radiation were inhibitable. Water transport did not inactivate with radiation; however, the inhibitory potency of 2.5 mM pCMBS decreased from 86 ± 1% to 4 ± 9% over a 0–2 Mrad dose range. These studies suggest that red cell water transport either required one or more low-molecular-weight proteins, or is lipid-mediated, and that the pCMBS-binding site which regulates water flow inactivates with radiation. These results also suggest that red cell urea transport is mediated by a specific, high-molecular-weight protein. These results do not support the hypothesis that a band 3 dimer (190 kDa) mediates red cell osmotic water and urea transport.

Introduction

Urea and water transport in human red cells has been studied extensively by stopped-flow and tracer techniques [1–4]. Despite this work, the molecular mechanisms of transport and the nature of the membrane components responsible for transport are not known. Both urea transport and, to a lesser extent, water transport are thought to require membrane proteins [1,5–8]; the identification of these proteins has not been unambiguous. Water transport may involve membrane lipids as well as membrane proteins [9,10], although the extent and mechanism by which water permeates by a lipid pathway have not been established.

We used radiation inactivation to explore the nature and molecular weight of osmotic water and urea pathways in the human red cell. Radiation inactivation has the advantage that the molecular properties of red cell water and urea transporters could be probed in intact cells, without isolation or purification of the transporters, which might alter native function or possible subunit assemblies [11,12]. We find that urea transport is characterized by a single target size of 469 ± 36 kDa, which establishes a lower limit to the molecular weight of the transport unit. Surprisingly, osmotic

* To whom correspondence and reprint requests should be addressed.

Abbreviation: Hepes, 4-(2-hydroxyethyl)-1-piperazineethanesulfonic acid.

water transport did not inactivate with radiation, however the ability of pCMBS to inhibit water transport disappears over a 0–2 Mrad radiation dose range. These findings support a protein pathway for urea in red cells, but suggest that water transport is either mediated entirely by lipid, by a small protein, or by a leak around or through a large protein; inhibition of water transport by mercurials may be regulated by a large inhibitor protein.

Methods

Radiation inactivation

Fresh human red cells obtained by venipuncture were washed three times in 150 mM NaCl/5 mM Hepes at pH 7.4. Packed cells were suspended in an equal volume of cryoprotectant solution containing 280 g glycerol/28 g sorbitol/720 ml of 150 mM NaCl/5 mM Hepes and equilibrated for 30 min at 4°C [13]. 1.5-ml aliquots of the suspension were rapidly frozen onto 1-mm deep aluminum trays by immersion in liquid nitrogen.

The frozen cells were placed in an aluminum chamber which was flushed for 3 min with liquid N_2 to replace air with a nitrogen atmosphere. The irradiation chamber was continuously cooled with flowing liquid N_2 to maintain sample temperature constantly in the range -45 to -52°C. Samples were irradiated with 1.5 MeV electrons generated from a Van de Graaf accelerator with a 0.5 mA beam current. The radiation dose was adjusted by varying the number of passages of the electron beam across the sample. Dosimetry was performed using Blue Cellophane foil (Dupont, dimethoxydiphenylbisazobis(8-amino-1-naphthol-5,7-disulfonic acid)) as described previously [14].

After irradiation, cells were thawed over 5 min by placing each aluminum tray upright in a glass tube. Cells were diluted in 30 ml of a 1:1 mixture of cryoprotectant solution and 150 mM NaCl/5 mM Hepes at pH 7.4, 4°C. Cells were centrifuged at $500 \times g$ for 5 min and resuspended in 600 mM NaCl/5 mM Hepes. The centrifugation/resuspension procedure was repeated in 300 mM NaCl/5 mM Hepes and in 150 mM sodium chloride/5 mM Hepes at pH 7.4. The final cell pellet was washed once and suspended in 150 mM NaCl/5 mM Hepes (pH 7.4) at approx. 2% hematocrit.

Red cell recovery was maximized using the procedure described above which consists of four washes of successively lower osmolarities. Fewer steps resulted in excessive hypotonic cell lysis, while additional steps decreased cell recovery because of mechanical trauma during pelleting and partial loss of the pellet during multiple aspirations. Cell recovery was generally between 30 and 60%. Since red cell ghost membranes are not pelleted by $500 \times g$, 5- min centrifugation, the final sample contained only intact, sealed red cells. Even if a small population of sealed red cell ghost membranes remained, the observed light-scattering signal would represent changes in size of intact red cells only, since red cell ghosts scatter light approx. 10-fold less than do intact red cells. As described in results, the freezing and thawing process had no effect on the rates of red cell osmotic water or urea transport, or on the inhibition of water transport by pCMBS and the inhibition of urea transport by phloretin.

Permeability measurements

Red cell osmotic water and urea permeability measurements were carried out at 25°C on a Dionex-130 stopped-flow apparatus (Sunnyvale, CA) interfaced to a Digital Equipment Corporation MINC/23 computer (Maynard, MA). Red cells in 150 mM NaCl/5 mM Hepes (pH 7.4) were mixed with hyperosmotic solutions to give a 200 mosM or a 500 mosM inwardly directed gradient of NaCl or a 500 mosM inwardly directed gradient of urea. The time-course of 90° scattered light at 500 nm was measured.

In studies involving transport inhibitors, the inhibitor was present in both the red cell and hyperosmotic solutions at the time of mixing. pCMBS was incubated with red cells for 30 min at 25°C in osmotic water transport experiments; control experiments showed that these conditions were sufficient for maximal inhibition. Phloretin and thiourea were added immediately before mixing in urea transport measurements.

Calculations

For osmotic water transport measurements in red cells, the time-course of cell volume normalized to initial cell volume, $V(t)$, is described by the

differential equation [2,15,16]:

$$\frac{d\hat{V}(t)}{dt} = \frac{A\tilde{v}_w P_f}{V_0}\left[\frac{C_i^0}{\hat{V}_{os}(t)} - C_o\right] \quad (1)$$

where A is the red cell surface area ($1.37 \cdot 10^{-6}$ cm^2 [17], V_0 is initial cell volume ($1.04 \cdot 10^{-10}$ cm^3 [17]), $\tilde{v}_w$ is the partial molar volume of water, P_f is the osmotic water permeability coefficient, C_i^0 is the initial intracellular impermeant concentration, and C_o is the solution-impermeant concentration which is constant in the limit of low hematocrit. $\hat{V}_{os}(t)$ is the osmotic water content of the red cell, defined by the relations:

$$\hat{V} = (1-b)V_{os} + b \quad (2)$$

$$\hat{V}_{os}(t) = V_{os}(t)/V_{os}(t=0) \quad (3)$$

The parameter b is the fraction of cell volume that does not participate in osmotic shrinkage, and is equal to 0.46 [2]. The relation between cell volume and scattered-light intensity, $I(t)$, is:

$$I(t) = \alpha V(t) + \beta \quad (4)$$

The observed time-course, $I(t)$, was fit by Eqns. 1–4 above using the nonlinear least-squares procedure, with P_f, α and β as fitted parameters. The shape of $I(t)$ predicted by Eqns. 1–4 is similar to that of a single exponential function for small osmotic perturbations.

The expression for $I(t)$ using a urea concentration gradient is more complex, since intracellular urea changes with time and a solvent drag term is required. Based on the equations of Kedem and Katchalsky [2,18], the time-course of cell volume is described by:

$$\frac{d\hat{V}_w}{dt} = \frac{A\tilde{v}_w P_f C_s^0}{V_w^0}\left[\frac{C_i^0}{C_s^0}\left(\frac{1}{\hat{V}_{os}(t)} - 1\right) + \sigma\left(\frac{\hat{n}_s}{\hat{V}_w} - 1\right)\right] \quad (5)$$

$$\frac{d\hat{n}_s}{dt} = \frac{AP_s'}{V_w^0}\left[1 - \frac{\hat{n}_s}{\hat{V}_w} + \left(\frac{1-\sigma}{2}\right)\left(1 + \frac{\hat{n}_s}{\hat{V}_w}\right)\frac{d\hat{V}_w}{dt}\right] \quad (6)$$

where C_s^0 is the extracellular permeant concentration and σ is the reflection coefficient. $\hat{V}_w$ is the cell water content, normalized to the initial cell water content, defined as:

$$\hat{V} = (1-f)V_w + f \quad (7)$$

$$\hat{V}_w = V_w(t)/V_w^0 \quad (8)$$

The parameter f is the fraction of cell volume that is cell solids, and is equal to 0.283 [19]. $\hat{n}_s$ is the number of moles of permeant present in the intracellular compartment, normalized to that present at infinite time:

$$\hat{n}_s = n_s/n_s^\infty = C_i V_w / C_s^0 V_w^0 \quad (9)$$

Since urea transport is characterized by saturable kinetics, the apparent urea permeability coefficient, P'_s, can be related to the true (0 concentration) permeability coefficient, P_{urea}, by [1,3]:

$$P_s' = P_{urea}/\left(1 + \left(C_s^0/K_m\right)\left(\hat{n}/\hat{V}_w\right)\right) \quad (10)$$

The value of K_m is taken to be 0.1 molar [1,3]. In writing these equations, we have assumed that the extracellular permeant concentration does not change with time, and that the permeant can partition into the total cell water volume.

The relation between cell volume, intracellular impermeant concentration and scattered-light intensity is:

$$I(t) = \alpha\left(\hat{V} + \delta\hat{n}_s/\hat{V}\right) + \beta \quad (11)$$

where the term $\delta\hat{n}_s/\hat{V}_w$ arises from the index of fraction change with intracellular urea concentration.

A fit of $I(t)$ to Eqns. 5–11 requires a six-parameter regression where P_f, P_{urea}, σ, α, δ and β are fitted parameters. Under the best of circumstances, such a regression is barely possible [1]. Experimentally, the signal-to-noise ratio of the light-scattering time-course decreases at higher radiation doses, requiring increased electronic filtering to eliminate random signal noise. Since water movement occurs on a much faster time-scale than urea movement and therefore requires less filtering, it was not practical to study both osmotic water and urea transport in a single measurement.

It is possible, however, to obtain an excellent approximation to the value for P_{urea} by fitting the measured $I(t)$ to a single exponential function:

$$I(t) = C\exp(-t/\tau) + D \quad (12)$$

where τ is the exponential time-constant, C is the amplitude and D is the baseline offset. Numerically generated time-courses, $I_{th}(t)$, were calcu-

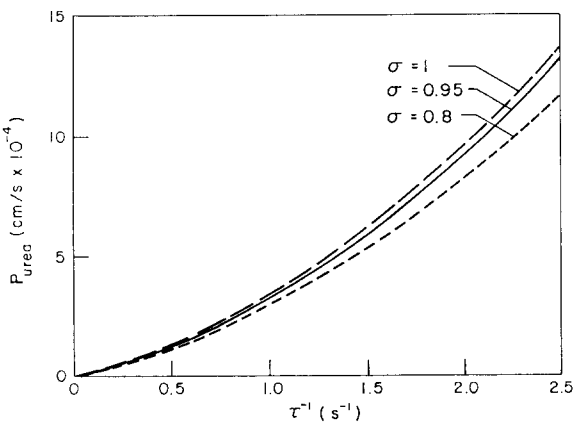

Fig. 1. Calculation of P_{urea} from exponential time-constants. For each value of P_{urea} and σ, $I(t)$ was generated numerically using Eqns. 5–11. $I(t)$ consisted of an increase in scattered-light intensity (water efflux) followed by a decrease in scattered light (urea influx). The phase of decreased scattering was fitted to a single exponential function (Eqn. 12). The fitted reciprocal exponential time-constant is plotted on the abscissa. Parameters: $V_0 = 1.4 \cdot 10^{-10}$ cm^3, $A = 1.37 \cdot 10^{-6}$ cm^2, $P_f = 0.02$ cm/s, $\bar{v}_w = 18$ cm^3/mol, $C_x^0 = 500$ mosM, $C_i^0 = 290$ mosM, $b = 0.46$, $f = 0.283$, $\delta = 0.01$ and $K_m = 100$ mM.

lated using Eqns. 5–11 for a series of P_{urea} and σ values. The phase of urea transport (decreased light scattering) in $I_{th}(t)$ was fit to a single-exponential function. The fitted reciprocal exponential time-constants are shown in Fig. 1 for a series of P_{urea} and σ values. Fig. 1 can thus be used to determine P_{urea} based on measured τ^{-1}. Since the curve is insensitive to the value of σ in the range reported for human red cells [1], τ^{-1} measurements are adequate to estimate P_{urea}. The curve in Fig. 1 is also insensitive to the value of δ in Eqn. 10; variation of δ by 25% had virtually no effect on the fitted time-constant.

Target sizes were calculated from the fitted slope, $-1/D_0$, of a ln(activity) vs. dose plot using the relation [11]:

$$\text{molecular mass} = -640/D_0 \text{ kDa} \quad (13)$$

where D_0 is the radiation dose, in Mrad, required to produce 37% inactivation. The accuracy of Eqn. 13 was confirmed using the present radiation inactivation technique from a calibration of known molecular mass vs. D_0 values for a series of enzymes, including horse liver alcohol dehydrogenase (84 kDa), yeast alcohol dehydrogenase (160 kDa), pyruvate kinase (224 kDa) and *Escherichia coli* β-galactosidase (464 kDa; Ref. 20) In addition, Eqn. 13 was found to be accurate for the molecular mass of alkaline phosphatase in rabbit renal brush-border vesicles [21], and acetylcholinesterase in human erythrocytes [22].

Results

The upper traces in Fig. 2 show the time-course of osmotic water and urea permeation in unirradiated red cells which have been frozen, stored and thawed in the same manner as the irradiated samples; the lower traces show the effect of transport inhibitors. As reported previously, pCMBS is an inhibitor of red cell osmotic water transport [6] and phloretin is an inhibitor of urea transport [5]. In order to freeze red cells, it was necessary to replace the solution buffer with a cryoprotectant solution used by Cuppoletti et al. [13] for target analysis studies of the red cell glucose transporter. As shown in Table I, the cryoprotection process has no effect on the rates of water or urea transport, nor on the inhibitory potency of pCMBS on water transport and of phloretin on urea transport. Furthermore, Cuppoletti et al. have shown that the cryoprotection process and radiation exposure (0–4 Mrad) had little effect on the integrity of red cell membranes as efficient permeability barriers; the half-time for equilibration of impermeant L-glucose was over 2 h at 25°C at a 4 Mrad radiation dose.

The effect of radiation on the time-course of

TABLE I

EFFECT OF RED CELL FREEZING AND THAWING ON OSMOTIC WATER AND UREA TRANSPORT

Inhibitors: water transport, 2.5 mM pCMBS; urea transport, 250 μM phloretin.

	No inhibitor (cm/s)	+ Inhibitor (% inhibition)
Water transport (P_f)		
Fresh	0.018 ± 0.001	83 ± 2
Frozen/thawed	0.020 ± 0.001	86 ± 2
Urea transport (P_{urea})		
Fresh	$(7.5 \pm 0.4) \cdot 10^{-4}$	95 ± 2
Frozen/thawed	$(6.0 \pm 0.3) \cdot 10^{-4}$	93 ± 2

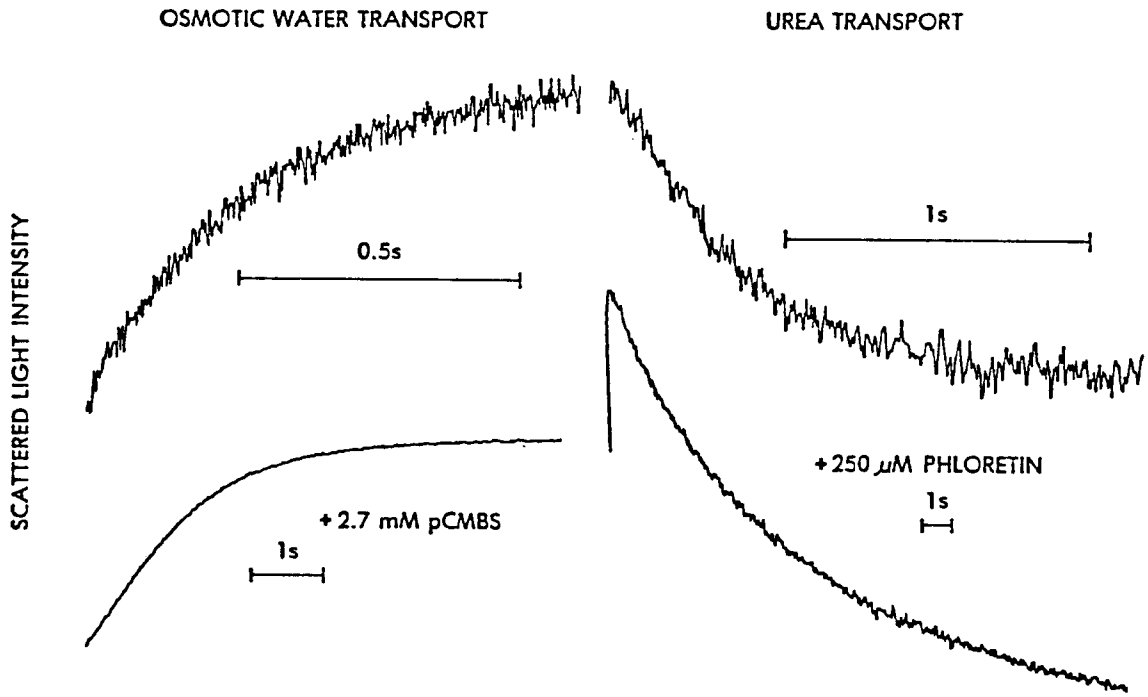

Fig. 2. Inhibitor effects on time-course of red cell water and urea transport in frozen/thawed cells. Left: The increase in light scattering (decreased red cell volume) is shown following imposition of a 500 mosM inwardly directed NaCl gradient with and without pCMBS. Data were fitted to Eqns. 1–4 with $P_f = 0.02$ cm/s (−pCMBS) and 0.0028 cm/s (+pCMBS). Right: After imposition of a 500 mM inwardly directed urea gradient, there is a rapid rise in light scattering (shown partially) followed by a slower decrease (red cell volume increase) due to urea influx. Fitted exponential time-constants are 0.66 s (−phloretin) and 9.4 s (+phloretin).

red cell osmotic water and urea transport is shown in Fig. 3. While there is little effect of radiation on osmotic water flow, urea transport slows considerably with increasing radiation. The ln(transport rate) vs. dose relations are shown in Fig. 4. For red cell osmotic water transport (Fig. 4, top), there is little change in P_f with radiation. The value of P_f extrapolated to 0 Mrad is 0.022 ± 0.002 cm/s, in good agreement with the recent P_f determinations by Terwilliger and Solomon (0.025 cm/s, Ref. 4) and Mlekoday et al. (0.020 cm/s, Ref. 2).

In contrast to water transport, urea transport exhibits a striking inactivation with radiation (Fig. 4, bottom); the inactivation is linear, with a target

TABLE II

INHIBITION OF RED CELL UREA TRANSPORT BY PHLORETIN AND THIOUREA

% Inhibition values represent the average of three measurements. Errors represent 1 S.D.

Dose (Mrad)	% Inhibition	
	40 μM phloretin	20 mM thiourea
0	47± 6	79± 6
1.9	44± 8	52± 8
3.1	41±11	64± 8
3.5	76±12	80±19

TABLE III

INHIBITION OF RED CELL OSMOTIC WATER TRANSPORT BY *p*-CHLOROMERCURIBENZENESULFONATE

Conditions: 2.5 mM pCMBS, 25°C, 30 min incubation.

Dose (Mrad)	% Inhibition
0	86±2
0.4	86±4
1.1	65±4
2.1	4±9
3.3	6±6

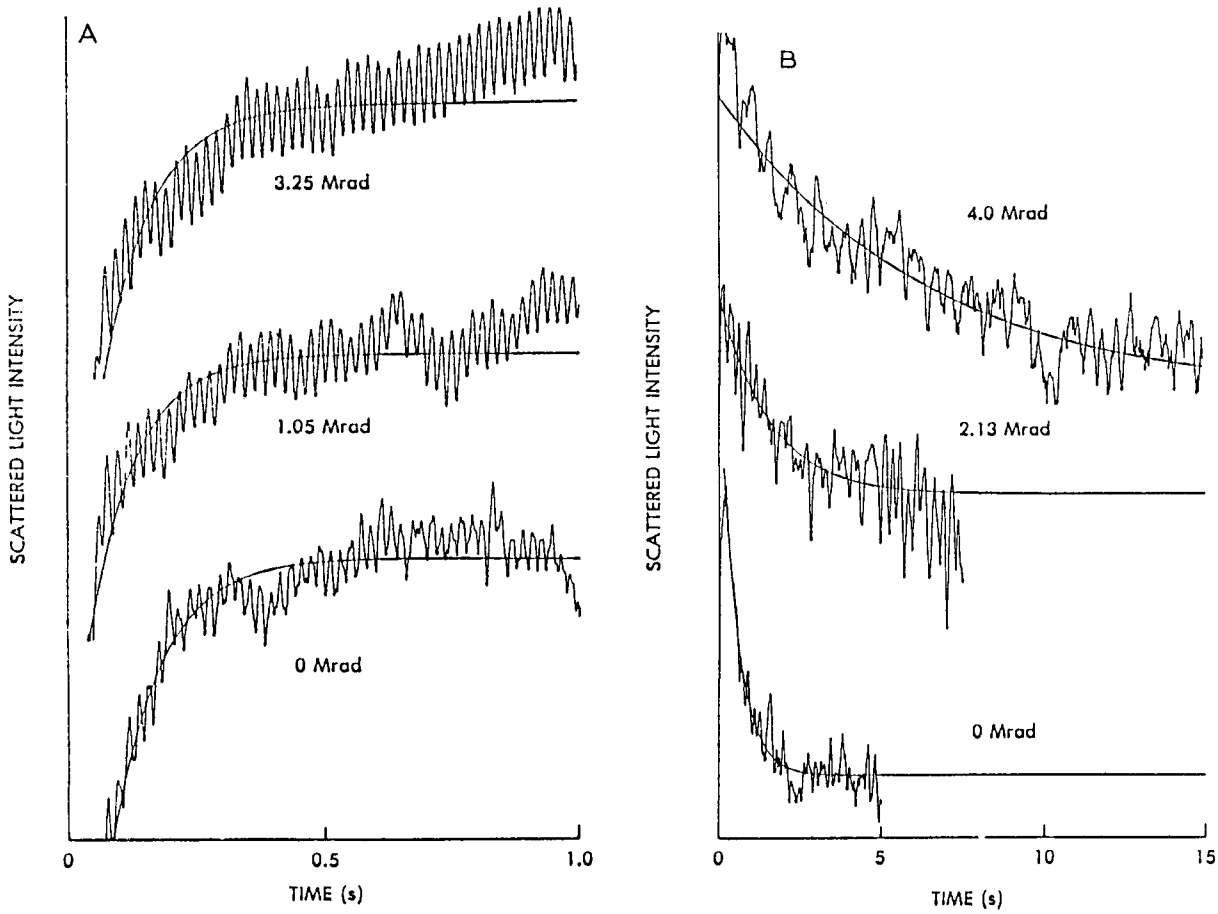

Fig. 3. Effect of radiation on the time-course of red cell water and urea transport. (A) Each time-course corresponds to a 500 mosM NaCl gradient at 25°C. Fitted P_f values are 0.019 cm/s (0 Mrad), 0.02 cm/s (1.05 Mrad) and 0.019 cm/s (3.25 Mrad). (B) Each time-course corresponds to a 500 mM urea gradient at 25°C. Fitted exponential time-constants are 0.55 s (0 Mrad), 2.1 s (2.13 Mrad) and 6.5 s (4 Mrad).

size of 469 ± 36 kDa. The value of P_{urea}, extrapolated to 0 Mrad is $(7.8 \pm 0.1) \cdot 10^{-4}$ cm/s, in agreement with the value of P_{urea} of $8.3 \cdot 10^{-4}$ cm/s determined by Levitt and Mlekoday [3].

In order to demonstrate that the urea transport activity surviving radiation has the same characteristics as urea transport in unirradiated red cells, the inhibitory effects of 40 μM phloretin and 20 mM thiourea were studied (Table II). There was no systematic deviation in the inhibitory potency of phloretin and thiourea on red cell urea transport as a function of radiation dose. In fact, the target size for red cell urea transport obtained in the presence of phloretin, 390 ± 73 kDa, and thiourea, 475 ± 100 kDa, did not differ significantly from the target size obtained for uninhibited urea transport.

Table III shows that the inhibitory potency of pCMBS for red cell osmotic water transport decreases from 86% to approx. 5% over a 0–2 Mrad dose range. Therefore, although osmotic water transport does not inactivate with radiation, the pCMBS inhibition site does. This surprising finding is explored further in discussion.

Discussion

Urea transport

There is strong evidence that a protein carrier facilitates urea transport in red cells. Urea trans-

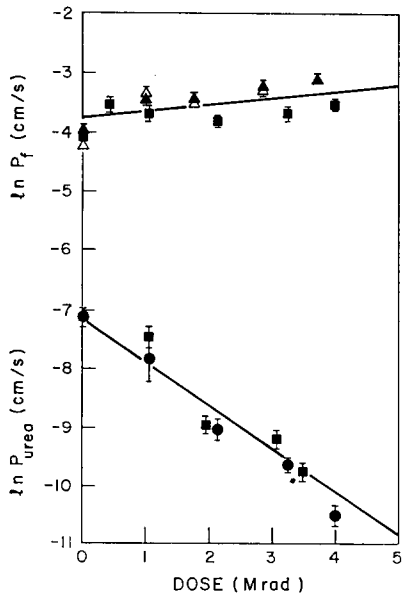

Fig. 4. Target analysis of red cell water and urea transport. Each data point is the average of three or more permeability coefficients, P_f, for osmotic water transport and P_{urea} for urea transport; error bars represent 1 S.D. Data points for water transport were obtained using either a 200 mosM (open triangles) or a 500 mosM (closed triangles and closed squares, different sets of experiments) osmotic gradient. Data points for urea transport are shown for two independent sets of experiments (solid squares and circles). Fitted slopes: 0.11 ± 0.07 $Mrad^{-1}$ (water) and -0.73 ± 0.04 $Mrad^{-1}$ (urea). The corresponding target size for urea transport is 469 ± 36 kDa.

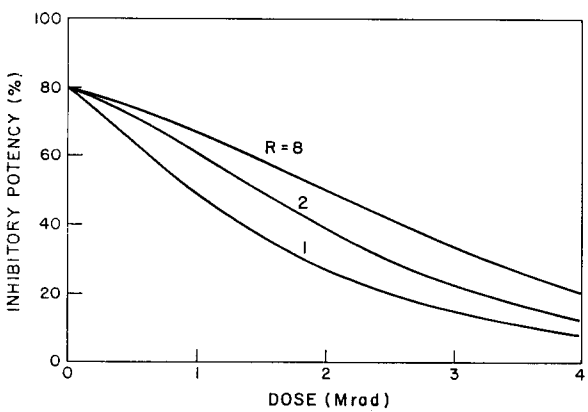

Fig. 5. Computer model for loss of pCMBS inhibitory potency with radiation. Curves were drawn from Eqn. A-11 using $1/D_W = 0$, $1/D_I = 0.63$ (400 kDa target size), indicated R values and K values chosen to give 80% inhibition in the absence of radiation. For $R = 1$, 2 and 8; $K = 0.05$, 0.3 and 1.8, respectively.

port is characterized by carrier-mediated kinetics, specific inhibition by pCMBS and phloretin and competition with urea analogues [1,6]. In addition, the permeability coefficient of urea in red cells is three orders of magnitude greater than that in lipid bilayers [22].

Although much is known about the rates, thermodynamics and inhibitory properties of red cell urea transport, the biochemical structure and molecular weight of the purported urea transport protein has not been determined. We find a target size for urea transport of 469 ± 36 kDa, consistent with a protein pathway for urea transport. In addition, since a single target size for inactivation was measured both in the absence and presence of inhibitors of urea transport, the urea transport consists of a functionally homogeneous population of membrane proteins.

How does the target size of the red cell urea transporter relate to its molecular weight? In a large series of enzymes, the target size determined by radiation inactivation was identical to the molecular weight determined by classical biochemical techniques; for a few enzymes composed of multiple subunits, the target size was smaller than the enzyme molecular mass and probed only the active subunit [11]. Therefore, the total molecular mass of the urea transporter may be greater than, but not less than 469 kDa. It may not be possible to identify the urea transporter on a gel electrophoresis of red cell membrane proteins, since there may be too few copies to measure. Target analysis gives no information about the number of urea transporters per red cell. Furthermore, if the urea transporter is a multimeric enzyme, then only individual subunits of molecular mass less than 469 kDa would be identified by gel electrophoresis.

Solomon et al. [7] have proposed that a dimer of a major glycoprotein of the red cell, band 3, is the urea transport protein. Band 3 is a transmembrane protein of 95 kDa, present in about 10^6 copies per cell, and is implicated as the anion transport protein [23]. If a dimer of band 3 were the urea transport unit, then radiation inactivation studies would yield a target size no larger than the molecular mass of the band 3 dimer, 190 kDa. Recently, the target size for band 3 has been estimated in three ways using the present radiation inactivation technique and method of dosimetry.

Jung, C.Y. (unpublished data) has measured the target size for both the anion-transport function and the loss of band 3 staining on an SDS electrophoretic gel and found an approx. 200 kDa target size for both. Verkman et al. (Verkman, A.S., Skorecki, K.L., Jung, C.Y. and Ausiello, D.A., unpublished data) confirmed these results and measured a 40 kDa target size for stilbene binding stoichiometry to human erythrocyte ghost membranes. Since the target size for urea transport is much larger than 180 kDa, our data do not support the proposition that a band 3 dimer is the urea transport unit. However, these results do not rule out involvement of band 3 in urea transport; recent evidence [24–25] suggests that band 3 may exist as a higher multimer in the red cell membrane, with a correspondingly higher molecular weight. If the target sites were composed of band 3 monomers, then a target size of 469 kDa would correspond to five band 3 monomers.

Water transport

Water transport in red cells is thought to occur either by bulk diffusion through an aqueous channel [7] or by single-file diffusion through a narrow channel [10]. Both models are consistent with an observed ratio of osmotic-to-diffusion permeability coefficients greater than unity. The organic mercurial, pCMBS, maximally inhibits 50% of the diffusional water transport and 90% of the osmotic water transport [6,26]. The water transport remaining after maximal pCMBS inhibition has characteristics similar to those of water transport in lipid bilayers, suggesting that water transport remaining after maximal pCMBS inhibition occurs through red cell lipids [9]. Since pCMBS is a sulfhydryl reagent known to bind to membrane proteins, the implication is that 50% of diffusional water transport and 90% of osmotic water transport occurs through a membrane protein pathway. The red cell protein or proteins responsible for water transport have not been identified, although, based on competition studies between pCMBS and anion-transport inhibitors known to bind to band 3 [27], it has been proposed that dimers of band 3 form an aqueous channel through which water transport occurs [7].

Our results do not support a large-molecular-weight-protein pathway for water transport through the red cell membrane, since red cell osmotic water transport, of which 90% is supposedly through a protein pathway, did not inactivate with radiation (Fig. 4). These results do not rule out a protein transport unit for water transport, however. Water transport may occur by an active monomeric subunit in equilibrium with a large inactive oligomer; in this model, a plot of ln(activity) vs. dose is concave downward. Under certain conditions, Verkman et al. [28,29] have shown that the slope of ln(activity) vs. dose plot may be nearly zero at low radiation doses. Therefore, if this model were correct, the downward curvature in the data might not be apparent at the relatively low radiation doses used. The highest radiation dose used was 4 Mrad, since excessive cell lysis was observed at higher doses.

A second possible interpretation for the data in Fig. 4 is that red cell water transport occurs primarily through red cell lipids; the target size of lipids is too small to be probed by radiation inactivation experiments. A single lipid pathway for red cell water transport is unlikely, based on the observed osmotic-to-diffusional permeability coefficient which is much greater than unity. Furthermore, Dix and Solomon [30] found no evidence for water transport through red cell lipids when the lipophilic anesthetic, halothane, was used to probe lipid pathways.

Although red cell osmotic water transport did not inactivate with radiation, the inhibitory potency of 2.5 mM pCMBS decreased from 86% inhibition in the absence of radiation to virtually no inhibition at 2 Mrad. These results have several possible interpretations. pCMBS may bind to a target distinct from the water transport pathway. Benga and colleagues [26] reached a similar conclusion from nuclear magnetic resonance studies of red cell diffusional water permeability. They found that papain digestion of red cell proteins strongly reduced the inhibitory potency of pCMBS, but had no effect on the magnitude of diffusional water flow. If the targets for pCMBS binding and osmotic water transport are distinct, and if there is a one-to-one coupling between inhibitory site occupancy and transport inhibition, the minimal target size for the pCMBS-binding site is 400 kDa (see Appendix). If, however, more than one inhibitory site is required for inhibition of a single water

transport channel, then the target size for the pCMBS-binding site could be much smaller. Therefore, the quantitative decrease in percent inhibition with radiation in Table III does not give precise information about the target size of the pCMBS-binding site.

There are two other possible interpretations for the observed loss of pCMBS inhibition with increasing radiation. There may be a single large protein which both transports water and binds pCMBS. The functional unit for water transport may be small, whereas intactness of the complete protein may be required for pCMBS binding and inhibition of water transport. In general, however, radiation does not destroy a partial function of a protein, making this possibility relatively unlikely.

On the basis of the present data, it is not possible to exclude a non-specific effect of radiation on the pCMBS-binding site. Radiation may destroy membrane sulfhydryl groups necessary for pCMBS binding by free radical formation, without destruction of the pCMBS-binding protein. We feel that this possibility is also unlikely, since samples are irradiated at $-50°C$, where free radical diffusion is minimal. In addition, the erythrocyte ghost pCMBS-binding site which is not reactive with *N*-ethylmaleimide has been probed by the radiation inactivation technique using tryptophan fluorescence to assay the binding site. The measured target size was 39 kDa (Verkman, A.S. et al., unpublished data), much smaller than the estimated target size for the pCMBS-binding site involved in water transport inhibition. Therefore, destruction of membrane pCMBS-binding sites at low radiation dose is not a general feature of sulfhydryl-binding sites.

In summary, red cell urea transport inactivates exponentially with radiation with a target size much larger than the size of a band 3 dimer. These data implicate the existence of a urea carrier in the red cell and represent the first estimate of its functional molecular mass. There is little effect of radiation on osmotic water transport, suggesting that the functional size of the 'water carrier' is quite small. Bulk water transport through an aqueous pore or single-file diffusion through a narrow channel are equally consistant with our results.

Appendix

In this Appendix, we formulate a model to examine one possible meaning of the loss of pCMBS inhibitory potency with increasing radiation. It is assumed that water transport sites, W, and inhibitory sites, I, are free to interact according to the mechanism:

$$\mathrm{pCMBS} + \mathrm{I} \leftrightarrow \mathrm{I_p} \leftrightarrow \underset{\swarrow\ \mathrm{W}}{\mathrm{W\text{-}I_p}} \qquad \text{(A-1)}$$

where I_p is an activated inhibitory site which is capable of binding to W to form an inactive W-I_p complex and inhibit water transport.

The mechanism is defined by two equilibrium constants:

$$K_I = [W][I_p]/[W\text{-}I_p] \qquad \text{(A-2)}$$

$$K_p = [pCMBS][I]/[I_p] \qquad \text{(A-3)}$$

and two conservation relations:

$$W_t = [W] + [W\text{-}I_p] \qquad \text{(A-4)}$$

$$I_t = [I] + [I_p] + [W\text{-}I_p] \qquad \text{(A-5)}$$

where W_t and I_t represent total site stoichiometries at any radiation dose, D, which are related to total site stoichiometries before radiation, W_t^0 and I_t^0, by the relations:

$$W_t = W_t^0 \exp(-D/D_W) \qquad \text{(A-6)}$$

$$I_t = I_t^0 \exp(-D/D_I) \qquad \text{(A-7)}$$

where D_W and D_I are radiation doses required to reduce initial site stoichiometry to 37% of its original value.

The % inhibition as used in Table III is defined by:

$$\%\ \text{inhibition} = 100\,(1 - [W]/W_t) \qquad \text{(A-8)}$$

Combining Eqns. A-2–A-8 and introducing the dimensionless parameters:

$$K = K_I(1 + K_p/[pCMBS])/W_t \qquad \text{(A-9)}$$

$$R = (I_t/W_t)\exp[-D(1/D_I - 1/D_W)] \qquad \text{(A-10)}$$

the required equation becomes:

$$\% \text{ inhibition} = 100\left(1 - 0.5\left[(1 - R - K) + \sqrt{(1 - R - K)^2 + 4K}\right]\right) \quad \text{(A-11)}$$

Fig. 5 shows the decrease in % inhibition with increasing radiation for several R values using target sizes of 0 and 400 kDa for the W and I sites, respectively. K has been chosen to give 80% inhibitory potency in the absence of radiation. As R increases, or equivalently, as the I:W site stoichiometry increases, it is necessary to choose a larger target size for I in order to predict a rapid decrease of % inhibitory potency with radiation as required by the data in Table III. Based on the model given in Eqn. A-1, a 400 kDa target size for I is the minimal size for I consistent with the data given in Table III.

Acknowledgements

We wish to thank Sarah Finnegan for technical assistance. Supported in part by NIH HL29488, AM35124 and AM27045.

References

1 Mayrand, R.R. and Levitt, D.G. (1983) J. Gen. Physiol. 81, 221–237
2 Mlekoday, H.J., Moore, R. and Levitt, D.G. (1983) J. Gen. Physiol. 81, 213–220
3 Levitt, D.G. and Mlekoday, H.J. (1983) J. Gen. Physiol. 81, 239–253
4 Terwilliger, T.C. and Solomon, A.K. (1981) J. Gen. Physiol. 77, 549–570
5 Wieth, J.O., Funder, J., Gunn, R.B. and Brahm, J. (1974) In Comparative Biochemistry and Physiology of Transport (Bolis, L., Block, K., Luria, S.E. and Lynan, F., eds.), pp. 317–337, Elsevier/North-Holland Biomedical Press, Amsterdam
6 Macey, R.I. and Farmer, R.E.L. (1970) Biochim. Biophys. Acta 211, 104–106
7 Solomon, A.K., Chasan, B., Dix, J.A., Lukacovic, M.F., Toon, M.R. and Verkman, A.S. (1983) Ann. N.Y. Acad. Sci. 414, 79–124
8 Brown, P.A., Feinstein, M.B. and Sha'afi, R.I. (1975) Nature (Lond.) 254, 523–525
9 Macey, R.I., Karan, D.M. and Farmer, R.E.L. (1972) in Passive Permeability of Cell Membranes: Biomembranes, Vol. III (Kreuzer, F. and Slegers, J.F.G., eds.), pp. 331–340, Plenum Press, New York
10 Macey, R.I. (1984) Am. J. Physiol. 246, C195–C203
11 Kempner, E.S. and Schlegel, W. (1979) Anal. Biochem. 92, 2–10
12 Kempner, E.S., Miller, J.H., Schlegel, W. and Hearon, J.Z. (1980) J. Biol. Chem. 255, 6826–6831
13 Cuppoletti, J., Jung, C.Y. and Green, F.A. (1981) J. Biol. Chem. 256, 1305–1306
14 Fricke, H. and Hart, E.J. (1966) in Radiation Dosimetry (Attix, R.H. and Rosche, W.C. eds.), Vol. 11, pp. 167–239, Academic Press, New York
15 Levitt, D.G. (1974) Biochim. Biophys. Acta 373, 115–131
16 Verkman, A.S., Dix, J.A. and Seifter, J.L. (1985) Am. J. Physiol. 248, F650–F655
17 Jay, A.W.L. (1975) Biophys. J. 15, 205–222
18 Kedem, O. and Katchalsky, A. (1958) Biochim. Biophys. Acta 27, 229–246
19 Savitz, D., Sidel, V. and Solomon, A.K. (1964) J. Gen. Physiol. 48, 79–91.
20 Ventner, J.C., Fraser, C.M., Schaber, J.S., Jung, C.Y., Bolger, G. and Triggle, D.J. (1983) J. Biol. Chem. 258, 9344–9348
21 Verkman, A.S., Dix, J.A., Seifter, J.L., Skorecki, K.L., Jung, C.Y. and Ausiello, D.A. (1985) Am. J. Physiol. 249, in the press
22 Gallucci, E., Micelli, S. and Lippe, C. (1971) Arch. Int. Physiol. Biochim. 79, 881–887
23 Knauf, P. (1979) Curr. Top. Membranes Trans. 12, 249–363
24 Jennings, M.L. (1984) J. Membrane Biol. 80, 105–117
25 Benz, R., Tosteson, M.T. and Schubert, D. (1984) Biochim. Biophys. Acta 775, 347–355
26 Benga, G., Popescu, O. and Pop, V.I. (1983) Cell Biol. Int. Rep. 7, 807–818
27 Lukacovic, M.F., Verkman, A.S., Dix, J.A. and Solomon, A.K. (1984) Biochim. Biophys. Acta 778, 253–259
28 Verkman, A.S., Skorecki, K. and Ausiello, D.A. (1984) Proc. Natl. Acad. Sci. USA 81, 150–154
29 Verkman, A.S., Skorecki, K. and Ausiello, D.A. (1986) Am. J. Physiol., in the press
30 Dix, J.A. and Solomon, A.K. (1984) Biochim. Biophys. Acta 773, 219–230